



Cooperative Computation of Stereo Disparity

D. Marr; T. Poggio

Science, New Series, Vol. 194, No. 4262. (Oct. 15, 1976), pp. 283-287.

Stable URL:

<http://links.jstor.org/sici?sici=0036-8075%2819761015%293%3A194%3A4262%3C283%3ACCORD%3E2.0.CO%3B2-1>

Science is currently published by American Association for the Advancement of Science.

Your use of the JSTOR archive indicates your acceptance of JSTOR's Terms and Conditions of Use, available at <http://www.jstor.org/about/terms.html>. JSTOR's Terms and Conditions of Use provides, in part, that unless you have obtained prior permission, you may not download an entire issue of a journal or multiple copies of articles, and you may use content in the JSTOR archive only for your personal, non-commercial use.

Please contact the publisher regarding any further use of this work. Publisher contact information may be obtained at <http://www.jstor.org/journals/aaas.html>.

Each copy of any part of a JSTOR transmission must contain the same copyright notice that appears on the screen or printed page of such transmission.

The JSTOR Archive is a trusted digital repository providing for long-term preservation and access to leading academic journals and scholarly literature from around the world. The Archive is supported by libraries, scholarly societies, publishers, and foundations. It is an initiative of JSTOR, a not-for-profit organization with a mission to help the scholarly community take advantage of advances in technology. For more information regarding JSTOR, please contact support@jstor.org.

Summary

The ability to directly measure and evaluate ultrafast processes with unprecedented time resolution and reliability has greatly extended our knowledge about the kinetics of primary processes in chemistry and allied physical and biological sciences. Improvements in the reliability and versatility of picosecond techniques should lead to an increase in the experimental information about basic interactions in atomic and molecular systems.

References and Notes

1. P. M. Rentzepis, *Chem. Phys. Lett.* **2**, 37 (1968).
2. D. Huppert, thesis, Tel-Aviv University, Ramat-Aviv, Israel (1975); — and P. M. Rentzepis, in *Molecular Energy Transfer*, R. D. Levine and J. Jortner, Eds. (Wiley, New York, 1975), p. 278.
3. K. B. Eisenthal, *Acc. Chem. Res.* **8**, 118 (1975); K. J. Kaufmann and P. M. Rentzepis, *ibid.*, p. 407; A. Lauberau and W. Kaiser, *Annu. Rev. Phys. Chem.* **26**, 83 (1975); R. R. Alfano and S. L. Shapiro, *Phys. Today* **1975**, 30 (July 1975).
4. P. W. Smith, M. A. Duguay, E. P. Ippen, *Prog. Quantum Electron.* **3**, 1 (1974).
5. M. R. Topp, P. M. Rentzepis, R. P. Jones, *J. Appl. Phys.* **42**, 3451 (1971).
6. R. R. Alfano and S. L. Shapiro, *Phys. Rev. Lett.* **24**, 584 (1970); G. E. Busch, P. M. Rentzepis, R. P. Jones, *Chem. Phys. Lett.* **18**, 178 (1973).
7. D. Huppert, K. Straub, E. O. Degenkolb, P. M. Rentzepis, in preparation.
8. K. S. Greve and G. E. Busch, in preparation.
9. C. V. Shank, *Rev. Mod. Phys.* **47**, 649 (1975).
10. H. E. Lessing, E. Lippert, W. Rapp, *Chem. Phys. Lett.* **7**, 247 (1970).
11. C. Lin, T. K. Gustafson, A. Dienes, *Opt. Commun.* **8**, 210 (1973).
12. D. N. Dempster, T. Morrow, R. Rankin, G. F. Thompson, *J. Chem. Soc. Faraday Trans. 2* **68**, 1479 (1972).
13. P. M. Rentzepis, R. P. Jones, J. Jortner, *J. Chem. Phys.* **54**, 766 (1973).
14. G. A. Kenney-Wallace and C. D. Jonah, *Chem. Phys. Lett.* **39**, 596 (1976).
15. D. Huppert, W. S. Struve, P. M. Rentzepis, J. Jortner, *J. Chem. Phys.* **63**, 1205 (1973).
16. D. Magde and M. W. Windsor, *Chem. Phys. Lett.* **24**, 144 (1974).
17. E. P. Ippen, C. V. Shank, A. Bergman, *ibid.* **38**, 611 (1976).
18. T. Förster and G. Hoffman, *Z. Phys. Chem. Neue Folge* **75**, 63 (1971).
19. J. F. Ireland and P. A. H. Wyatt, *Adv. Phys. Org. Chem.* **12**, 131 (1976).
20. D. von der Linde and K. F. Rodgers, *IEEE J. Quantum Electron.* **QE-9**, 960 (1973).
21. G. E. Busch, M. L. Applebury, A. Lamola, P. M. Rentzepis, *Proc. Natl. Acad. Sci. U.S.A.* **69**, 2802 (1972).
22. T. L. Netzel, P. M. Rentzepis, J. Leigh, *Science* **182**, 238 (1973).
23. J. S. Leigh, Jr., T. L. Netzel, P. L. Dutton, P. M. Rentzepis, *FEBS Lett.* **48**, 136 (1974).
24. K. J. Kaufmann, P. L. Dutton, T. L. Netzel, J. S. Leigh, P. M. Rentzepis, *Science* **188**, 1301 (1975).
25. M. G. Rockley, M. M. Windsor, R. J. Cogdell, W. W. Parson, *Proc. Natl. Acad. Sci. U.S.A.* **72**, 2251 (1975).
26. W. W. Parson, R. K. Clayton, R. J. Cogdell, *Biochim. Biophys. Acta* **387**, 265 (1975).
27. K. J. Kaufmann, K. M. Petty, P. L. Dutton, P. M. Rentzepis, *Biochem. Biophys. Res. Commun.* **70**, 839 (1976).
28. P. L. Dutton, K. J. Kaufmann, B. Chance, P. M. Rentzepis, *FEBS Lett.* **60**, 275 (1975).
29. T. L. Netzel, P. L. Dutton, P. M. Rentzepis, in preparation.
30. M. Seibert and R. R. Alfano, *Biophys. J.* **14**, 269 (1974).
31. W. Yu, P. P. Ho, R. R. Alfano, M. Seibert, *Biochim. Biophys. Acta* **387**, 159 (1975).
32. S. L. Shapiro, V. H. Kollman, A. J. Campillo, *FEBS Lett.* **54**, 358 (1975).
33. See, for example, J. B. Birks, *Photophysics of Aromatic Molecules* (Wiley-Interscience, New York, 1970), pp. 567–590.
34. D. Huppert, P. M. Rentzepis, G. Tollin, *Biochim. Biophys. Acta* **440**, 356 (1976).
35. A. J. Campillo, S. L. Shapiro, V. H. Kollman, K. R. Winn, R. C. Hyer, *Biophys. J.* **16**, 93 (1976).
36. K. J. Kaufmann, P. M. Rentzepis, W. Stoeckenius, A. Lewis, *Biochem. Biophys. Res. Commun.* **68**, 1109 (1976).
37. D. Huppert, P. M. Rentzepis, D. Kliger, *Photochem. Photobiol.*, in press.
38. G. Wald, *Science* **162**, 230 (1968).
39. We thank Drs. P. L. Dutton, D. Huppert, and K. Kaufmann and K. S. Greve, G. Olson, and R. Ito for their many helpful contributions and discussions.

Cooperative Computation of Stereo Disparity

A cooperative algorithm is derived for extracting
disparity information from stereo image pairs.

D. Marr and T. Poggio

Perhaps one of the most striking differences between a brain and today's computers is the amount of "wiring." In a digital computer the ratio of connections to components is about 3, whereas for the mammalian cortex it lies between 10 and 10,000 (1).

Although this fact points to a clear structural difference between the two, this distinction is not fundamental to the nature of the information processing that each accomplishes, merely to the particulars of how each does it. In Chomsky's terms (2), this difference affects theories of performance but not theories of competence, because the nature of a computation that is carried out by a machine or a nervous system depends only on a problem to be solved, not on the avail-

able hardware (3). Nevertheless, one can expect a nervous system and a digital computer to use different types of algorithm, even when performing the same underlying computation. Algorithms with a parallel structure, requiring many simultaneous local operations on large data arrays, are expensive for today's computers but probably well-suited to the highly interactive organization of nervous systems.

The class of parallel algorithms includes an interesting and not precisely definable subclass which we may call cooperative algorithms (3). Such algorithms operate on many "input" elements and reach a global organization by way of local, interactive constraints. The term "cooperative" refers to the way in

which local operations appear to cooperate in forming global order in a well-regulated manner. Cooperative phenomena are well known in physics (4, 5), and it has been proposed that they may play an important role in biological systems as well (6–10). One of the earliest suggestions along these lines was made by Julesz (11), who maintains that stereoscopic fusion is a cooperative process. His model, which consists of an array of dipole magnets with springs coupling the tips of adjacent dipoles, represents a suggestive metaphor for this idea. Besides its biological relevance, the extraction of stereoscopic information is an important and yet unsolved problem in visual information processing (12). For this reason—and also as a case in point—we describe a cooperative algorithm for this computation.

In this article, we (i) analyze the computational structure of the stereo-disparity problem, stating the goal of the computation and characterizing the associated local constraints; (ii) describe a cooperative algorithm that implements this computation; and (iii) exhibit its performance on random-dot stereograms. Although the problem addressed here is not directly related to the question of

D. Marr is at the Artificial Intelligence Laboratory, Massachusetts Institute of Technology, Cambridge 02139. T. Poggio is at the Max-Planck Institut für Biologische Kybernetik, 74 Tübingen 1, Speimannstrasse 38, Germany.

how the brain extracts disparity information, we shall briefly mention some questions and implications for psychophysics and neurophysiology.

Computational Structure of the Stereo-Disparity Problem

Because of the way our eyes are positioned and controlled, our brains usually receive similar images of a scene taken from two nearby points at the same horizontal level. If two objects are separated in depth from the viewer, the relative positions of their images will differ in the two eyes. Our brains are capable of measuring this disparity and of using it to estimate depth.

Three steps (S) are involved in measuring stereo disparity: (S1) a particular location on a surface in the scene must be selected from one image; (S2) that same location must be identified in the other image; and (S3) the disparity in the two corresponding image points must be measured.

If one could identify a location beyond doubt in the two images, for example by illuminating it with a spot of light, steps S1 and S2 could be avoided and the problem would be easy. In practice one cannot do this (Fig. 1), and the difficult part of the computation is solving the correspondence problem. Julesz found that we are able to interpret random-dot stereograms, which are stereo pairs that consist of random dots when viewed monocularly but fuse when viewed stereoscopically to yield patterns separated in depth. This might be thought surprising, because when one tries to set up a correspondence between two arrays of random dots, false targets arise in profusion (Fig. 1). Even so, we are able to determine the correct correspondence. We need no other cues.

In order to formulate the correspondence computation precisely, we have to examine its basis in the physical world. Two constraints (C) of importance may be identified (13): (C1) a given point on a physical surface has a unique position in space at any one time; and (C2) matter is cohesive, it is separated into objects, and the surfaces of objects are generally smooth compared with their distance from the viewer.

These constraints apply to locations on a physical surface. Therefore, when we translate them into conditions on a computation we must ensure that the items to which they apply there are in one-to-one correspondence with well-defined locations on a physical surface. To do this, one must use surface markings,

normal surface discontinuities, shadows, and so forth, which in turn means using predicates that correspond to changes in intensity. One solution is to obtain a primitive description [like the primal sketch (14)] of the intensity changes present in each image, and then to match these descriptions. Line and edge segments, blobs, termination points, and tokens, obtained from these by grouping, usually correspond to items that have a physical existence on a surface.

The stereo problem may thus be reduced to that of matching two primitive descriptions, one from each eye. One can think of the elements of these descriptions as carrying only position information, like the white squares in a random-dot stereogram, although in practice there will exist rules about which matches between descriptive elements are possible and which are not. The two physical constraints C1 and C2 can now be translated into two rules (R) for how the left and right descriptions are combined:

R1) *Uniqueness*. Each item from each image may be assigned at most one disparity value. This condition relies on the assumption that an item corresponds to something that has a unique physical position.

R2) *Continuity*. Disparity varies smoothly almost everywhere. This condition is a consequence of the cohesiveness of matter, and it states that only a small fraction of the area of an image is composed of boundaries that are discontinuous in depth.

In real life, R1 cannot be applied simply to gray-level points in an image. The simplest counterexample is that of a goldfish swimming in a bowl: many points in the image receive contributions from the bowl and from the goldfish. Here, and in general, a gray-level point is in only implicit correspondence with a physical location, and it is therefore impossible to ensure that gray-level points in the two images correspond to exactly the same physical position. Sharp changes in intensity are usually due either to the goldfish, to the bowl, or to a reflection, and therefore define a single physical position precisely.

A Cooperative Algorithm

By constructing an explicit representation of the two rules, we can derive a cooperative algorithm for the computation. Figure 2a exhibits the geometry of the rules in the simple case of a one-dimensional image. L_x and R_x represent the positions of descriptive elements on

the left and right images. The thick vertical and horizontal lines represent lines of sight from the left and right eyes, and their intersection points correspond to possible disparity values. The dotted diagonal lines connect points of constant disparity.

The uniqueness rule R1 states that only one disparity value may be assigned to each descriptive element. If we now think of the lines in Fig. 2a as a network, with a node at each intersection, this means that only one node may be switched on along each horizontal or vertical line.

The continuity rule R2 states that disparity values vary smoothly almost everywhere. That is, solutions tend to spread along the dotted diagonals.

If we now place a "cell" at each node (Fig. 2b) and connect it so that it inhibits cells along the thick lines in the figure and excites cells along the dotted lines, then, provided the parameters are appropriate, the stable states of such a network will be precisely those in which the two rules are obeyed. It remains only to show that such a network will converge to a stable state. We were able to carry out a combinatorial analysis [as in (9, 15)] which established its convergence for random-dot stereograms (16).

This idea may be extended to two-dimensional images simply by making the local excitatory neighborhood two dimensional. The structure of each node in the network for two-dimensional images is shown in Fig. 2c.

A simple form of the resulting algorithm (3) is given by the following set of difference equations:

$$C^{(n+1)} = \sigma\{\Xi(C^{(n)}) + C^{(0)}\} \quad (1)$$

that is,

$$C_{xyd}^{(n+1)} = \sigma\left\{ \sum_{x'y'd' \in S(xyd)} C_{x'y'd'}^{(n)} - \epsilon \sum_{x'y'd' \in O(xyd)} C_{x'y'd'}^{(n)} + C_{xyd}^{(0)} \right\} \quad (2)$$

where $C_{xyd}^{(n)}$ represents the state of the node or cell at position (x,y) with disparity d at iteration n , Ξ is the linear operator that embeds the local constraints (S and O are the circular and thick line neighborhoods of the cell xyd in Fig. 2c), ϵ is the "inhibition" constant, and σ is a sigmoid function with range $[0, 1]$. The state $C_{xyd}^{(n+1)}$ of the corresponding node at time $(n+1)$ is thus determined by a nonlinear operator on the output of a linear transformation of the states of neighboring cells at time n .

The desired final state of the computation is clearly a fixed point of this al-

gorithm; moreover, any state that is inconsistent with the two rules is not a stable fixed point. Our combinatorial analysis of this algorithm shows that, when σ is a simple threshold function, the process converges for a rather wide range of parameter values (16). The specific form of the operator is apparently not very critical.

Noniterative local operations cannot solve the stereo problem in a satisfactory way (11). Recurrence and nonlinearity are necessary to create a truly cooperative algorithm that cannot be decomposed into the superposition of local operations (17). General results concerning such algorithms seem to be rather difficult to obtain, although we believe that one can usually establish convergence in probability for specific forms of them.

Examples of Applying the Algorithm

Random-dot stereograms offer an ideal input for testing the performance of the algorithm, since they enable one to bypass the costly and delicate process of transforming the intensity array received by each eye into a primitive description (14). When we view a random-dot stereogram, we probably compute a description couched in terms of edges rather than squares, whereas the inputs to our algorithm are the positions of the white

squares. Figures 3 to 6 show some examples in which the iterative algorithm successfully solves the correspondence problem, thus allowing disparity values to be assigned to items in each image. Presently, its technical applications are limited only by the preprocessing problem.

This algorithm can be realized by various mechanisms, but parallel, recurrent, nonlinear interactions, both excitatory and inhibitory, seem the most natural. The difference equations set out above would then represent an approximation to the differential equations that describe the dynamics of the network.

Implications for Biology

We have hitherto refrained from discussing the biological problem of how stereopsis is achieved in the mammalian brain. Our analyses of the computation, and of the cooperative algorithm that implements it, raise several precise questions for psychophysics and physiology. An important preliminary point concerns the relative importance of neural fusion and of eye movements for stereopsis. The underlying question is whether there are many disparity "layers" (as our algorithm requires), or whether there are just three "pools" (18)—crossed, uncrossed, and zero disparity. Most physi-

ologists and psychologists seem to accept the existence of numerous, sharply tuned binocular "disparity detectors," whose peak sensitivities cover a wide range of disparity values (19, 20). We do not believe that the available evidence is decisive (21), but an answer is critical to the biological relevance of our analysis. If, for example, there were only three pools or layers with a narrow range of disparity sensitivities, the problem of false targets is virtually removed, but at the expense of having to pass the convergence plane of the eyes across a surface in order to achieve fusion. Psychophysical experiments may provide some insight into this problem, but we believe that only physiology is capable of providing a clear-cut answer.

If this preliminary question is settled in favor of a "multilayer" cooperative algorithm, there are several obvious implications of the network (Fig. 2) at the physiological level: (i) the existence of many sharply tuned disparity units that are rather insensitive to the nature of the descriptive element to which they may refer; (ii) organization of these units into disparity layers (or stripes or columns); (iii) the presence of reciprocal excitation within each layer; and (iv) the presence of reciprocal inhibition between layers along the two lines of sight. Ideally, the inhibition should exhibit the characteristic "orthogonal" geometry of the thick

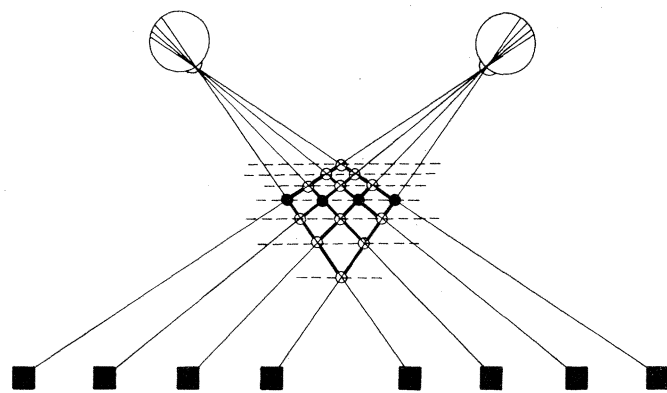
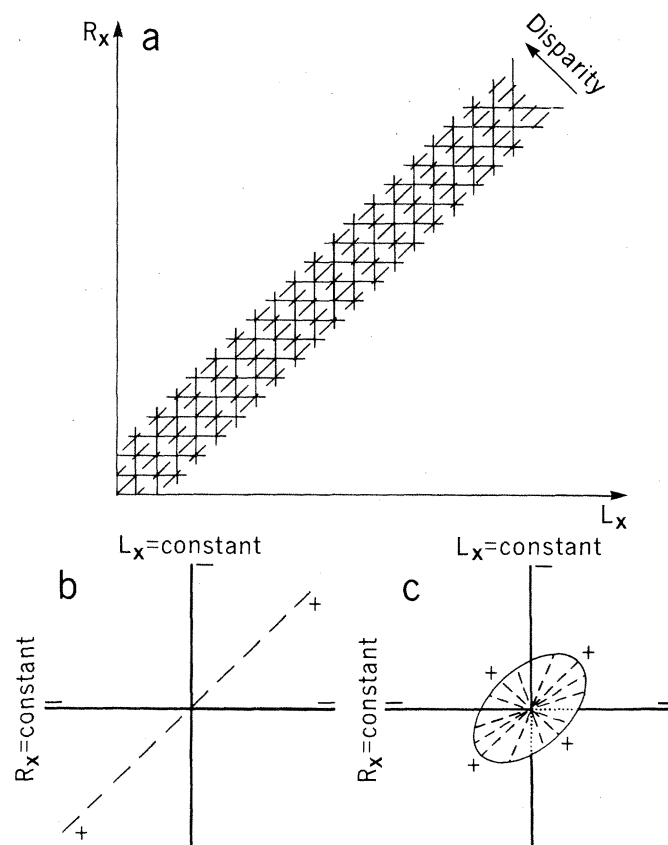


Fig. 1 (left). Ambiguity in the correspondence between the two retinal projections. In this figure, each of the four points in one eye's view could match any of the four projections in the other eye's view. Of the 16 possible matchings only four are correct (closed circles), while the remaining 12 are "false targets" (open circles). It is assumed here that the targets (closed squares) correspond to "matchable" descriptive elements obtained from the left and right images. Without further constraints based on global considerations, such ambiguities cannot be resolved. Redrawn from Julesz (11, figure 4.5-1). Fig. 2 (right). The explicit structure of the two rules R1 and R2 for the case of a one-dimensional image is represented in (a), which also shows the structure of a network for implementing the algorithm described by Eq. 2. Solid lines represent "inhibitory" interactions, and dotted lines represent "excitatory" ones. The local structure at each node of the network in (a) is given in (b). This algorithm may be extended to two-dimensional images, in which case each node in the corresponding network has the local structure shown in (c). Such a network was used to solve the stereograms exhibited in Figs. 3 to 6.



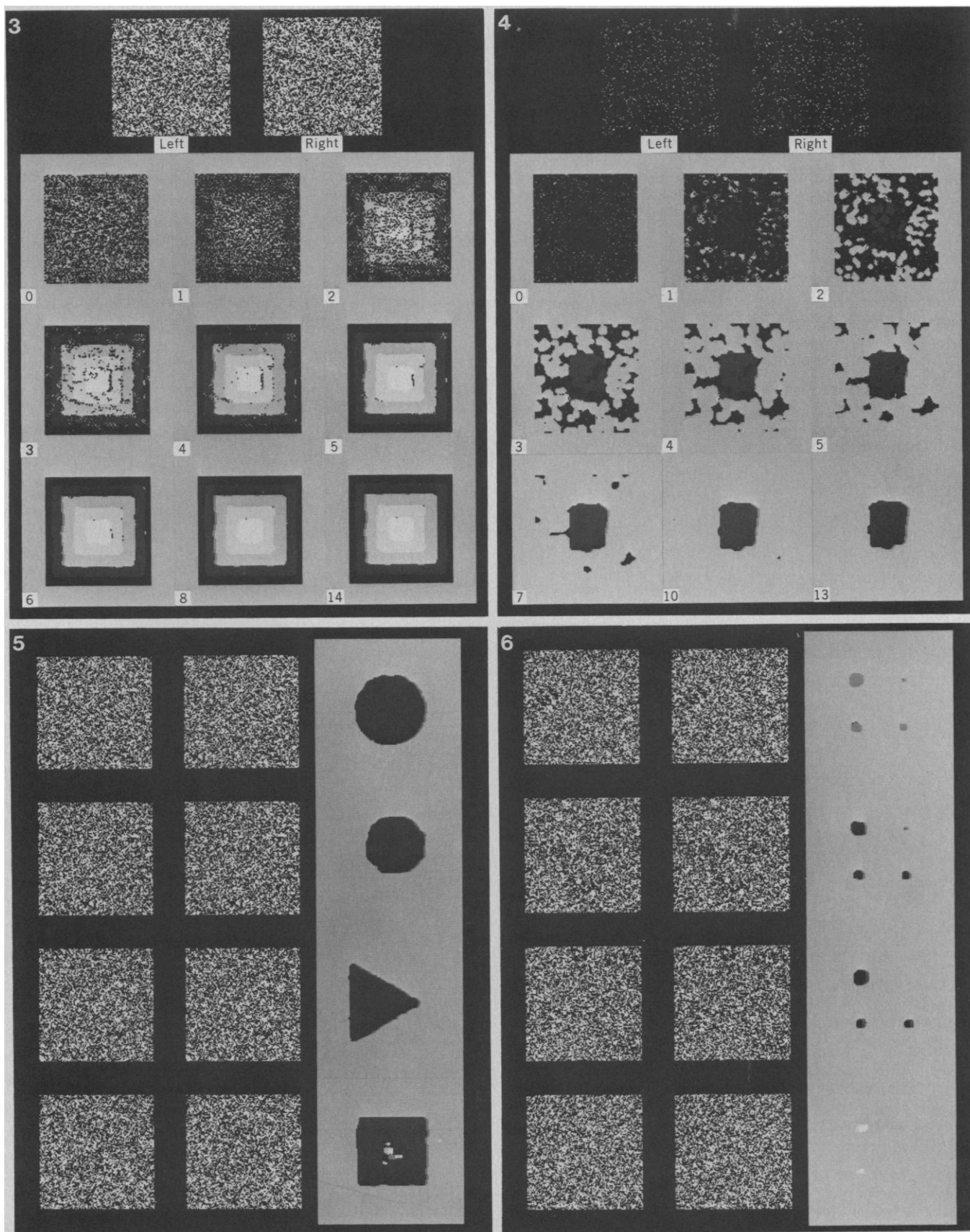
lines in Fig. 2, but slight deviations may be permissible (16).

At the psychophysical level, several experiments (under stabilized image conditions) could provide critical evidence for or against the network: (i) results

about the size of Panum's area and the number of disparity "layers"; (ii) results about "pulling" effects in stereopsis (20); and (iii) results about the relationship between disparity and the minimum fusible pattern size (Fig. 6).

Discussion

Our algorithm performs a computation that finds a correspondence function between two descriptions, subject to the two constraints of uniqueness and conti-



nunity. More generally, if one has a situation where allowable solutions are those that satisfy certain local constraints, a cooperative algorithm can often be constructed so as to find the nearest allowable state to an initial one. Provided that the constraints are local, use of a cooperative algorithm allows the representation of global order, to which the algorithm converges, to remain implicit in the network's structure.

The interesting difference between this stereo algorithm and standard correlation techniques is that one is not required to specify minimum or maximum correlation areas to which the analysis is subsequently restricted. Previous attempts at implementing automatic stereocomparison through local correlation measurement have failed in part because no single neighborhood size is always correct (12). The absence of a "characteristic scale" is one of the most interesting properties of this algorithm, and it is a central feature of several cooperative phenomena (22). We conjecture that the matching operation implemented by the algorithm represents in some sense a generalized form of correlation, subject to the a priori requirements imposed by the constraints. The idea can easily be generalized to different constraints and to other forms of equations 1 or 2,

and it is technically quite appealing.

Cooperative algorithms may have many useful applications [for example, to make best matches for associative retrieval problems (15)], but their relevance to early processing of information by the brain remains an open question (23). Although a range of early visual processing problems might yield to a cooperative approach ["filling-in" phenomena, subjective contours (24), grouping, figural reinforcement, texture "fields," and the correspondence problem for motion], the first important and difficult task in problems of biological information processing is to formulate the underlying computation precisely (3). After that, one can study good algorithms for it. In any case, we believe that an experimental answer to the question of whether depth perception is actually a cooperative process is a critical prerequisite to further attempts at analyzing other perceptual processes in terms of similar algorithms.

Summary

The extraction of stereo-disparity information from two images depends upon establishing a correspondence between them. In this article we analyze

the nature of the correspondence computation and derive a cooperative algorithm that implements it. We show that this algorithm successfully extracts information from random-dot stereograms, and its implications for the psychophysics and neurophysiology of the visual system are briefly discussed.

References and Notes

1. D. A. Sholl, *The Organisation of the Cerebral Cortex* (Methuen, London, 1956). The comparison depends on what is meant by a component. We refer here to the level of a gate and of a neuron, respectively.
2. A. N. Chomsky, *Aspects of the Theory of Syntax* (MIT Press, Cambridge, Mass., 1965).
3. D. Marr and T. Poggio, *Neurosci. Res. Prog. Bull.*, in press (also available as *Mass. Inst. Technol. Artif. Intell. Lab. Memo 357*).
4. H. Haken, Ed. *Synergetics-Cooperative Phenomena in Multicomponent Systems* (Teuber, Stuttgart, 1973).
5. H. Haken, *Rev. Mod. Phys.* **47**, 67 (1975).
6. J. D. Cowan, *Prog. Brain Res.* **17**, 9 (1965).
7. H. R. Wilson and J. D. Cowan, *Kybernetik* **13**, 55 (1973).
8. M. Eigen, *Naturwissenschaften* **58**, 465 (1971).
9. P. H. Richter, paper contributed to a competition of the Bavarian Academy of Science, Max-Planck-Institut für Biophysikalische Chemie, 1974.
10. A. Gierer and H. Meinhardt, *Kybernetik* **12**, 30 (1972).
11. B. Julesz, *Foundations of Cyclopean Perception* (Univ. of Chicago Press, Chicago, 1971).
12. K. Mori, M. Kidode, H. Asada, *Comp. Graphics Image Process.* **2**, 393 (1973).
13. D. Marr, *Mass. Inst. Technol. Artif. Intell. Lab. Memo 327* (1974).
14. ———, *Philos. Trans. R. Soc. London Ser. B* **275**, 483 (1976).
15. ———, *ibid.* **252**, 23 (1971). See especially section 3.1.2.
16. ——— and T. Poggio, in preparation.
17. T. Poggio and W. Reichardt, *Q. Rev. Biophys.*, in press.
18. W. Richards, *J. Opt. Soc. Am.* **62**, 410 (1971).
19. H. B. Barlow, C. Blakemore, J. D. Pettigrew, *J. Physiol. (London)* **193**, 327 (1967); J. D. Pettigrew, T. Nikara, P. O. Bishop, *Exp. Brain Res.* **6**, 391 (1968); C. Blakemore, *J. Physiol. (London)* **209**, 155 (1970).
20. B. Julesz and J.-J. Chang, *Biocybernetics* **22**, 107 (1976).
21. D. H. Hubel and T. N. Wiesel, *Nature (London)* **225**, 41 (1970).
22. K. G. Wilson, *Rev. Mod. Phys.* **47**, 773 (1975).
23. Julesz (11), Cowan (6), and Wilson and Cowan (7) were the first to discuss explicitly the cooperative aspect of visual information processing. Much has been published recently on possible cooperative processes in nervous systems, ranging from the "catastrophe" literature [E. C. Zeeman, *Sci. Am.* **234**, 65 (April 1976)] to various attempts of more doubtful credibility. There has hitherto been no careful study of a cooperative algorithm in the context of a carefully defined computational problem [but see (15)], although algorithms that may be interpreted as cooperative were discussed, for instance, by P. Dev [Int. J. Man-Mach. Stud. **7**, 511 (1975)] and by A. Rosenfeld, R. A. Hummel, and S. W. Zucker [Syst. Man. Cybern. **6**, 420 (1976)]. In particular neither Dev nor J. I. Nelson [J. Theor. Biol. **49**, 1 (1975)] formulated the computational structure of the stereo-disparity problem. As a consequence, the resulting geometry of the inhibition between their disparity detectors does not correspond to ours (Fig. 2c) and apparently fails to provide a satisfactory algorithm.
24. S. Ullmann, *Mass. Inst. Technol. Artif. Intell. Lab. Memo 367* (1967); also in *Biol. Cybern.*, in press.
25. We thank W. Richards for valuable discussions, H. Lieberman for making it easy to create stereograms, and K. Prendergast for preparing the figures. The research described was done at the Artificial Intelligence Laboratory of the Massachusetts Institute of Technology. Support for the laboratory's artificial intelligence research is provided in part by the Advanced Research Projects Agency of the Department of Defense under Office of Naval Research contract N00014-75-C-0643; T.P. acknowledges the support of the Max-Planck-Gesellschaft during his visit to the Massachusetts Institute of Technology.

Figs. 3 to 6. The results of applying the algorithm defined by Eq. 2 to two random-dot stereograms. Fig. 3. The initial state of the network $C^{(0)}$ is defined by the input such that a node takes the value 1 if it occurs at the intersection of a 1 in the left and right eyes (Fig. 2), and it has the value 0 otherwise. The network iterates on this initial state, and the parameters used here, as suggested by the combinatorial analysis, were $\theta = 3.0$, $\epsilon = 2.0$, and $M = 5$, where θ is the threshold and M is the diameter of the "excitatory" neighborhood illustrated in Fig. 2c. The stereograms themselves are labeled *Left* and *Right*, the initial state of the network as 0, and the state after n iterations is marked as such. To understand how the figures represent states of the network, imagine looking at it from above. The different disparity layers in the network lie in parallel planes spread out horizontally, so that the viewer is looking down through them. In each plane, some nodes are on and some are off. Each of the seven layers in the network has been assigned a different gray level, so that a node that is switched on in the top layer (corresponding to a disparity of +3 pixels) contributes a dark point to the image, and one that is switched on in the lowest layer (disparity of -3) contributes a lighter point. Initially (iteration 0) the network is disorganized, but in the final state stable order has been achieved (iteration 14), and the inverted wedding-cake structure has been found. The density of this stereogram is 50 percent. Fig. 4. The algorithm of Eq. 2, with parameter values given in the legend to Fig. 3, is capable of solving random-dot stereograms with densities from 50 percent to less than 10 percent. For this and smaller densities, the algorithm converges increasingly slowly. If a simple homeostatic mechanism is allowed to control the threshold θ as a function of the average activity (number of "on" cells) at each iteration [compare (15)], the algorithm can solve stereograms whose density is very low. In this example, the density is 5 percent and the central square has a disparity of +2 relative to the background. The algorithm "fills in" those areas where no dots are present, but it takes several more iterations to arrive near the solution than in cases where the density is 50 percent. When we look at a sparse stereogram, we perceive the shapes in it as cleaner than those found by the algorithm. This seems to be due to subjective contours that arise between dots that lie on shape boundaries. Fig. 5. The disparity boundaries found by the algorithm do not depend on their shapes. Examples are given of a circle, an octagon (notice how well the difference between them is preserved), and a triangle. The fourth example shows a square in which the correlation is 100 percent at the boundary but diminishes to 0 percent in the center. When one views this stereogram, the center appears to shimmer in a peculiar way. In the network, the center is unstable. Fig. 6. The width of the minimal resolvable area increases with disparity. In all four stereograms the pattern is the same and consists of five circles with diameters of 3, 5, 7, 9, and 13 dots. The disparity values exhibited here are +1, +2, +3, and +6, and for each pattern we show the state of the network after ten iterations. As far as the network is concerned, the last pair (disparity of +6) is uncorrelated, since only disparities from -3 to +3 are present in our implementation. After ten iterations, information about the lack of correlation is preserved in the two largest areas.